



# Development and Performance Evolution of Medium-Pressure He/SF<sub>6</sub>/O<sub>2</sub>-Based Plasma and Wet Chemical Etching Process for Surface Modification of Fused Silica

Hari Narayan Singh Yadav<sup>1</sup> · Manas Das<sup>1</sup>

Received: 25 October 2023 / Accepted: 10 January 2024 / Published online: 5 February 2024  
© The Author(s), under exclusive licence to Springer Science+Business Media, LLC, part of Springer Nature 2024

## Abstract

The rising demand for precision optics widely employed in ground and space-based astronomical instruments and other scientific instrumentation requires highly efficient advanced fabrication methods. Due to complex-shaped fused silica substrate surfaces like freeform or aspheres with strong curvatures or very small-sized components, a novel non-contact medium-pressure plasma-based method is developed to finish optical components. The present study critically compares the polished optical surfaces of a prism with a medium-pressure plasma process and wet chemical etching to provide insight into their smoothing. The results show that surface roughness ( $R_a$ ) increases from 0.54 to 2.61 nm and 0.53 to 0.57 nm at 5 and 20 mbar total pressures, respectively, using a plasma process without surface contamination. However, wet chemical etching increases surface roughness ( $R_a$ ) from 0.52 to 15.9 nm. The substrates' surface morphology, elemental composition, and surface topography are analyzed using FESEM, EDX, and AFM. Moreover, subsurface improvements are analyzed using Raman spectroscopy analysis.

**Keywords** Optical material · Plasma process · Wet chemical etching · Surface roughness · FESEM · Raman spectroscopy

## Abbreviations

FESEM	Field emission scanning electron microscopy
EDX	Energy dispersive X-ray
AFM	Atomic force microscopy
$R_a$	Surface roughness
UVL	Ultraviolet lithography
EUVL	Extreme ultraviolet lithography
APPP	Atmospheric pressure plasma polishing
RF	Radio-frequency

✉ Manas Das  
manasdas@iitg.ac.in

<sup>1</sup> Department of Mechanical Engineering, Indian Institute of Technology Guwahati, Assam 781039, India

PJM	Plasma jet machining
PAMM	Plasma-induced atom migration manufacturing
MPPP	Medium-pressure plasma polishing
MRR	Material removal rate
LIDT	Laser-induced damage threshold
OES	Optical emission spectrometer

## Introduction

Fused silica is utilized to fabricate optical components such as lenses, mirrors, photonic crystals, and prisms [1]. Fused silica is commonly used in precision devices due to its outstanding optical properties [2]. Surface finish, geometrical accuracy, and surface integrity necessities of optical components used primarily in inertial sensors such as accelerometers and gyros are challenging. However, its rigid and brittle properties make the components hard to process, as high surface quality is essential for manufacturing sectors and industries. The demand for good surface-quality optical substrates is growing because of the developments in the microelectronics and optics sectors [3]. Kogelschatz et al. [4] discussed the dielectric-barrier discharges and their uses, including their history, discharge physics, and plasma chemistry. Plasma polishing is an effective technique for ultra-smooth finishing of brittle and hard substrates such as glass, fused silica, sapphire, crystal, quartz, etc. [5]. Schindler et al. [6] proposed that high-performance optical components having aspherical surfaces, for instance, mirrors and lenses polished using plasma process, are becoming increasingly important for applications such as extreme ultraviolet lithography (EUVL), ultraviolet lithography (UVL), X-ray optical systems, and optical-satellite-communication components. Atmospheric pressure plasma polishing (APPP) is a non-contact machining method that removes atomic-scale material using low-temperature plasma chemical reactions [7]. APPP is a non-contact finishing process that is influenced by several factors. An initial theoretical study and simulation show that radio-frequency (RF) power, gas ratio, and working distance are significant parameters [8]. Yadav et al. [9] studied the distribution of electron density, temperature, and potential for differently shaped substrate surfaces in the plasma chamber by using Comsol Multiphysics® and found their dependency on the geometry of the substrate. Gerhard et al. [10] observed that the plasma process reduces surface scattering by significantly lowering the waviness and surface roughness of the substrate. Thomas et al. [11] utilized atmospheric pressure plasma jet machining to create and rectify freeform optical surfaces (i.e., made of fused silica) flexibly and effectively while smoothening or polishing the surfaces. Gerhard et al. [12] reported that the plasma treatment significantly reduces the transmission of the glass samples. Moreover, the ellipsometric analysis revealed a reduction in the superficial index of refraction of around 3.66% at a wavelength of 636.7 nm. Arnold et al. [13] reported that plasma jet machining (PJM) technology depends on deterministic plasma-assisted material removal. It can produce and rectify medium and small-sized optical complexes and freeform components. APPP techniques are used in industries to achieve the sub-nanometre level surface finish. Li et al. [14] reported that plasma-induced atom migration manufacturing (PAMM) produces large optical substrates with outstanding optical performance and long operational life. It can produce highly efficient damage-free surfaces at a cheap cost. The concentration of elements, i.e., Ce, K, and H, are determined in the adjacent surface layer of the finished samples

using secondary ion mass spectrometry [15]. However, these processes are not deterministic with respect to ‘zero surface defects’ and do not eliminate subsurface damages.

Dev et al. [16] developed a medium-pressure plasma polishing (MPPP) for polishing navigation-grade inertial sensors. The result reveals an ultrafine surface finish on the component’s surface with ‘zero’ surface or sub-surface damage. Yadav et al. [17] reported a highest 13% decrease in strained and damaged layers of fused silica using MPPP at optimal conditions, i.e., 90:10 gas composition (He: (SF<sub>6</sub>+O<sub>2</sub>)), 1:1 pressure ratio (SF<sub>6</sub>/O<sub>2</sub>), 20 mbar plasma chamber pressure. Yadav and Das [18] reported a 3.59% change in surface roughness and MRR of 0.012 mm<sup>3</sup>/min utilizing MPPP at optimized parameters, i.e., 60 W RF power, 3 pressure ratio, and 14.3 mbar total pressure using response surface methodology. MPPP integrates the advantages of low-pressure plasma etching, which includes isotropic material removal from all surfaces simultaneously via ions, with the characteristics of atmospheric plasma processes, emphasizing chemical vaporization over physical ion bombardment. Therefore to overcome these limitations, non-contact, medium-pressure plasma-based techniques are utilized to finish the optical components while achieving defect-free surfaces. The medium-pressure plasma process is conducted in a closed chamber inside a vacuum environment, unlike the atmospheric-pressure plasma process performed in an open environment (as reported in the literature). Hence, there is a rare chance of surface contaminations on fused silica substrate as no foreign particles are employed during the medium-pressure plasma process, unlike in the atmospheric pressure plasma process, where substrate surface contamination is a significant issue.

Wet chemical etching removes the damaged surface and subsurface layer, compromising the surface finish and significantly degrading the topography [16]. Feit et al. [19] revealed that fluoride-based wet chemical etching of fused silica optical substrate aids in opening surface cracks for diagnostic reasons, producing a surface topology, and as a potential mitigation strategy to remove damaged material. Cheng et al. [20] reported HF-based wet chemical etching and observed that the contamination is removed from fused silica. Experimental testing is carried out to assess the effectiveness of etching by examining defect content, surface quality, and laser damage threshold on the etched surfaces. Ye et al. [21] reported that HF etching does not impact hardness, and there is no observable correlation between the laser-induced damage threshold (LIDT) and hardness. Etching leads to a slight increase in the laser-induced damage threshold. However, deep etching could potentially decrease the LIDT. Nevertheless, the hardness remains nearly constant during both etching and deep etching processes. Ye et al. [22] observed the development of scratch morphologies and evaluated damage performance compared to surfaces without brittle scratches. The findings indicate that wet chemical etching leads to the expansion of the scratches, the opening of microcracks, and the blunting of their edges.

The present study compares the medium-pressure plasma process and wet chemical etching of a cuboidal-shaped prism made of fused silica to provide insight into their smoothing, i.e., surface roughness, morphology, and topography. The purpose of employing MPPP is to eliminate subsurface damage while ensuring the absence of surface contamination, specifically after removing the damaged layer from the surface. Subsurface damage (SSD) is an inherent defect resulting from mechanical processes like grinding and polishing.

In contrast to traditional mechanical machining methods, medium-pressure plasma processing (MPPP) is a relatively modern technology that causes minimal subsurface damage (SSD) when working with optical materials. The developed process aims to achieve a smooth surface finish on freeform surfaces while eliminating surface and subsurface damage. The atomistic material removal process has also led to decreased surface cracks,

thereby improving surface integrity. It possesses the capability to remove material from the workpiece at the atomic level without the formation of a heat-affected zone or the initiation of micro-cracks that lead to surface or subsurface damage. The process is deterministic for complex and free-form surfaces. The novelty of the present medium-pressure plasma process is negligible surface contamination over the atmospheric pressure plasma process. Also, the novelty of the present study is that it gives the advantage of the current medium-pressure plasma process over the other, i.e., medium-pressure plasma is better than wet chemical etching for the finishing of optical materials. In atmospheric pressure plasma, the polishing is conducted on a single spot, unlike the uniform polishing requirement over the entire surface in the medium-pressure plasma process (i.e., in the present study). An advantage of medium-pressure plasma is the lower probability of surface contamination while achieving the desired surface finish. This study can benefit industries and organizations in finishing optical materials without surface contamination while eliminating subsurface defects after removing the damaged layer from conventional machining. Also, the medium-pressure plasma process can substantially improve subsurface damage. The uniqueness of this process stems from its capacity to polish entire intricate 3D surfaces simultaneously, even in cavities inaccessible to conventional tools or beams. FESEM, EDX, and AFM are utilized to investigate surface morphology, elemental composition, and surface topography, respectively. Moreover, Raman microscopy is utilized to analyze improvement in the subsurface defects.

## Materials and Methods

This section provides an in-depth discussion of the mechanism of the plasma process, the experimental setup and specifications, process parameters, and the preparation of substrates for medium-pressure plasma and wet chemical etching. Furthermore, a detailed analysis of the system design for wet chemical etching is also presented.

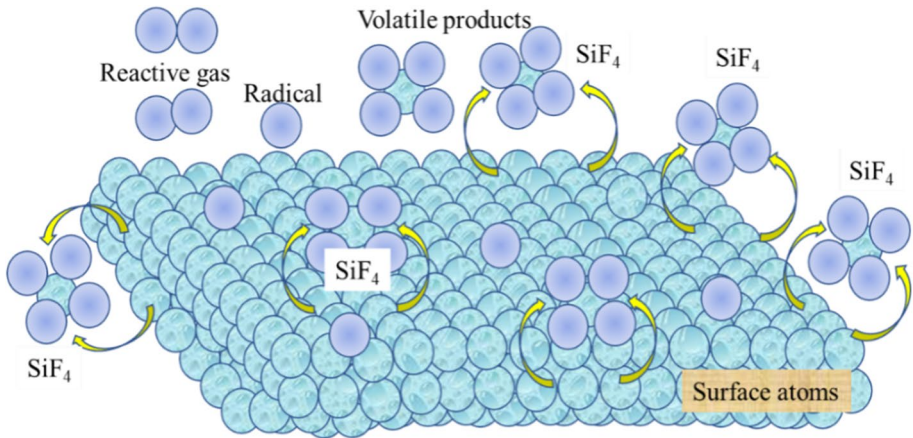
### Mechanisms of Plasma Process

An advanced, novel, and damage-free method, i.e., medium-pressure plasma, is utilized to polish optical materials. In the initial phase, the process chamber is filled with the auxiliary gases (He, O<sub>2</sub>) and the reactive gas (SF<sub>6</sub>) in an optimal ratio, followed by ionization through RF power. The gases are energized within the plasma chamber, generating reactive radicals, ions, etc. The generated radical causes a chemical reaction with the substrate surface, efficiently removing material at the atomic level. The reaction between a single fluorine radical and fused silica is illustrated in Eq. (1) [18]. The mechanism of the plasma polishing process is shown in Fig. 1.



### Experimental Setup of Plasma Process

MPPP is designed and developed for the uniform finishing of optical components up to 40 mm in length. The schematic and actual diagram of the MPPP system include a vacuum system and various gas units necessary for plasma processing, as presented in



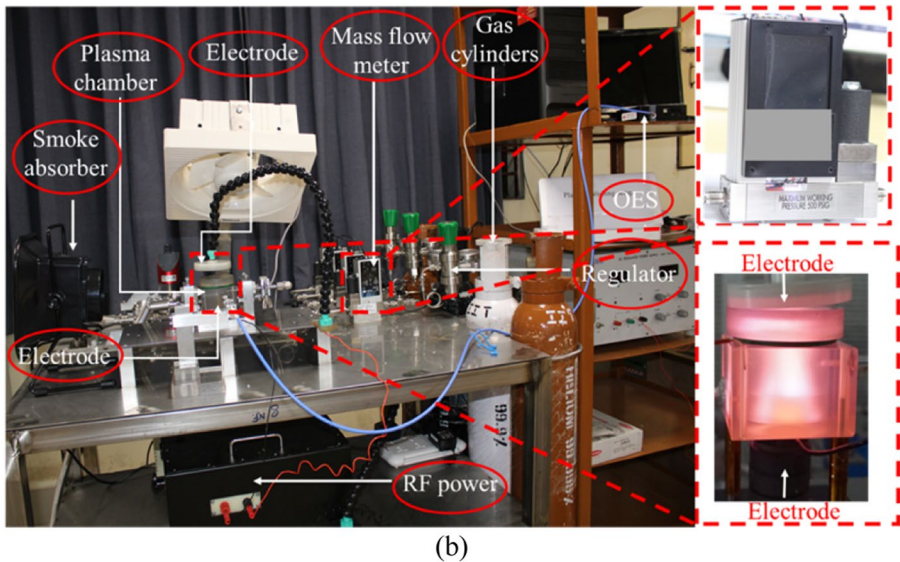
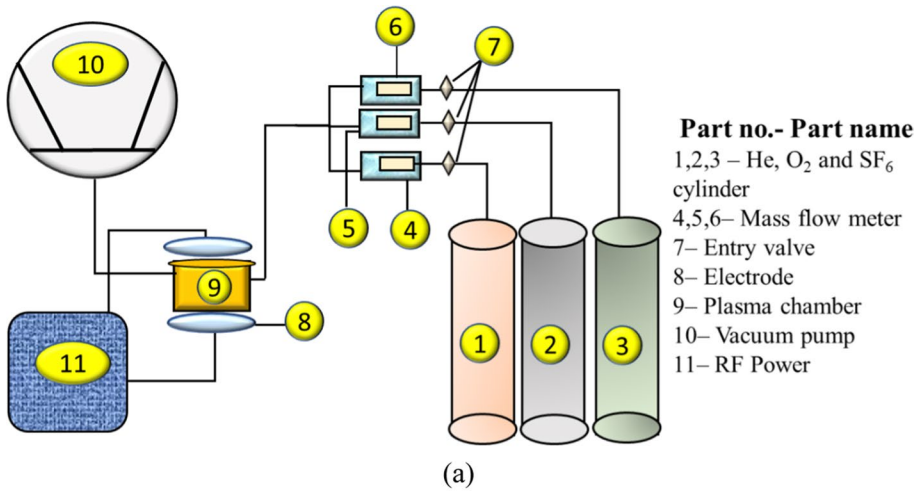
**Fig. 1** Mechanism of plasma polishing process

Fig. 2a and b, respectively. The plasma chamber is fabricated using zerodur material. The system comprises a vacuum pump and various gas-feeding lines that are linked to the plasma chamber. The electrodes are positioned externally to the plasma chamber and are not in touch with the plasma chamber, a unique aspect of this experimental setup, as shown in Fig. 2a with parts no. 8 & 9. Medium pressure is chosen for plasma processing to prevent ions from impacting the substrate. Furthermore, an RF excitation scheme with a dielectric barrier is employed to minimize electron heating and facilitate the chemical interaction of reactive free radicals with the surface atoms of the work-piece. An RF excitation frequency of 40.68 MHz is chosen to reduce ion bombardment to a minimum.

The plasma chamber is linked to the vacuum system and connected to three gas supply lines. The fiber optic probe head of the optical emission spectrometer is employed to measure the species' densities in the energized states, which is very useful for interpreting the mechanism of material processing under the plasma process. In MPPP, working gases, such as reactive gas, i.e., SF<sub>6</sub>, and processing gases (He, O<sub>2</sub>), are admitted into the process chamber. The specifications of the plasma processing setup and its operating parameters are illustrated in Tables 1 and 2, respectively.

## System Design for Wet Chemical Etching

Wet chemical etching is used to remove material from freeform and complex surfaces. Initially, the substrate is prepared using the traditional machining processes. The substrate is then dried at room temperature after being thoroughly cleaned in deionized water using an ultrasonic cleaner. Substrates are treated by being submerged in the solution of HF and H<sub>2</sub>SO<sub>4</sub> as illustrated in Fig. 3. During wet chemical etching, the etchant reacts with the material surface through various chemical reactions, including dissolution, oxidation, and reduction. During experiments, the fused silica substrate is subjected to wet chemical etching using a mixed solution consisting of hydrofluoric acid and sulfuric acid with a volume ratio of 2:1.



**Fig. 2** Medium-pressure plasma polishing experimental setup **a** schematic diagram and **b** actual setup

## Results and Discussion

This section discusses the polishing results of optical components before and after processing. A comparative study between the plasma process and wet chemical etching is also discussed.

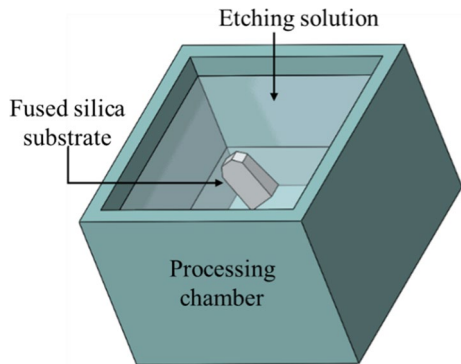
**Table 1** Specification of plasma processing setup

Gap between electrodes and plasma chamber	Plasma chamber body	Discharge frequency	Substrate material	Processing and reactive gases
1 to 2 mm	Zerodur	40.68 MHz	Fused silica	O <sub>2</sub> , He, and SF <sub>6</sub>



**Table 2** Process parameters of medium-pressure plasma process

Parameters	Range	Unit
RF power	80	W
SF <sub>6</sub> flow rate	1.9	sccm
O <sub>2</sub> flow rate	0.49	sccm
He flow rate	10	sccm
Chamber pressure	5 & 20	mbar
Processing time	40	mins

**Fig. 3** Schematic of wet chemical etching setup

### Qualitative Analysis of Plasma Discharge at Various Pressures and Power

Preliminary experiments involving the use of a helium (He) plasma are conducted to study and analyze the extent of plasma discharge occurring within a plasma chamber. Such experiments are often essential to understand the behavior of the plasma and gather important data before proceeding with more complex or detailed investigations. Experiments are conducted at varying pressures with different RF power to compare the plasma discharge within the plasma chamber. An increase in plasma discharge directly influences the plasma polishing process. A complete plasma discharge uniformly removes material from the substrate [13]. The removal of material from the substrate during processing depends on the quantity of discharge inside the plasma chamber. Figure 4 shows the qualitative measurement of plasma generation at various pressures inside the plasma chamber. Qualitative measurement of plasma generation refers to the assessment and description of the characteristics and properties of a plasma, typically without relying on precise numerical values or quantitative data. The author measures the discharge % by (1) observing the color and appearance of the plasma, which can provide information about its discharge percentage, (2) using spectroscopy to analyze the spectral lines and emission spectra of the plasma, (3) examining the visual patterns or shapes of the plasma. The experiments are repeated three times for every pressure, and the average value of these three measurements is calculated to get the response, i.e., discharge percentage. The flow rate (sccm) of He gas is measured corresponding to the individual plasma chamber pressure, as illustrated in Fig. 4.






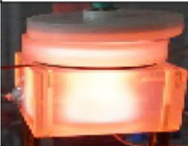

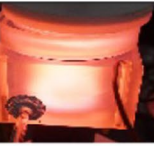



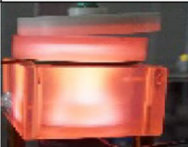





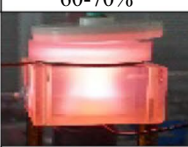



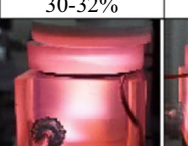
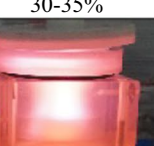
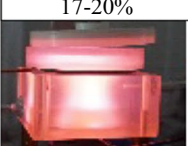
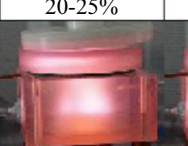
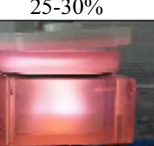
Pressure (mbar)	Flow rate (sccm)	Plasma discharge at various RF powers		
		20 W	40 W	80 W
5 mbar	8 sccm			
		80-85%	90-92%	100%
10 mbar	17 sccm			
		85-90%	92-95%	100%
15 mbar	32 sccm			
		90-92%	95-97%	100%
20 mbar	45 sccm			
		75-80%	80-82%	100%
30 mbar	80 sccm			
		60-70%	60-70%	60-70%
40 mbar	125 sccm			
		25-30%	30-32%	30-35%
50 mbar	177 sccm			
		17-20%	20-25%	25-30%
60 mbar	235 sccm			
		10-12%	12-14%	12-15%

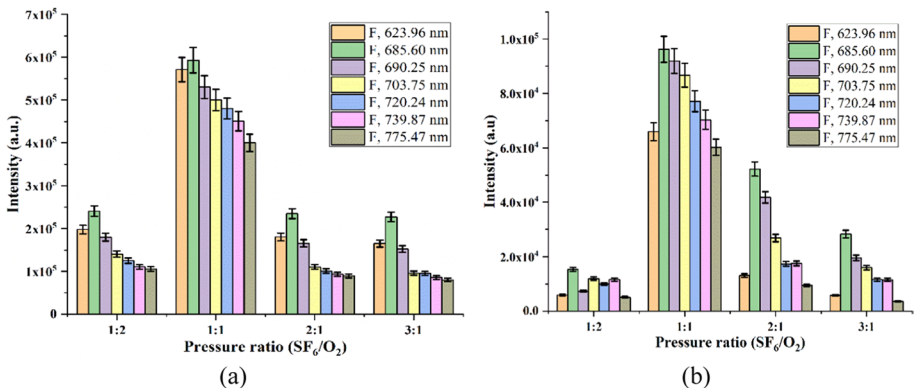
Fig. 4 Qualitative discharge percentage at various pressures and power

## Chemical Properties of Plasma Species

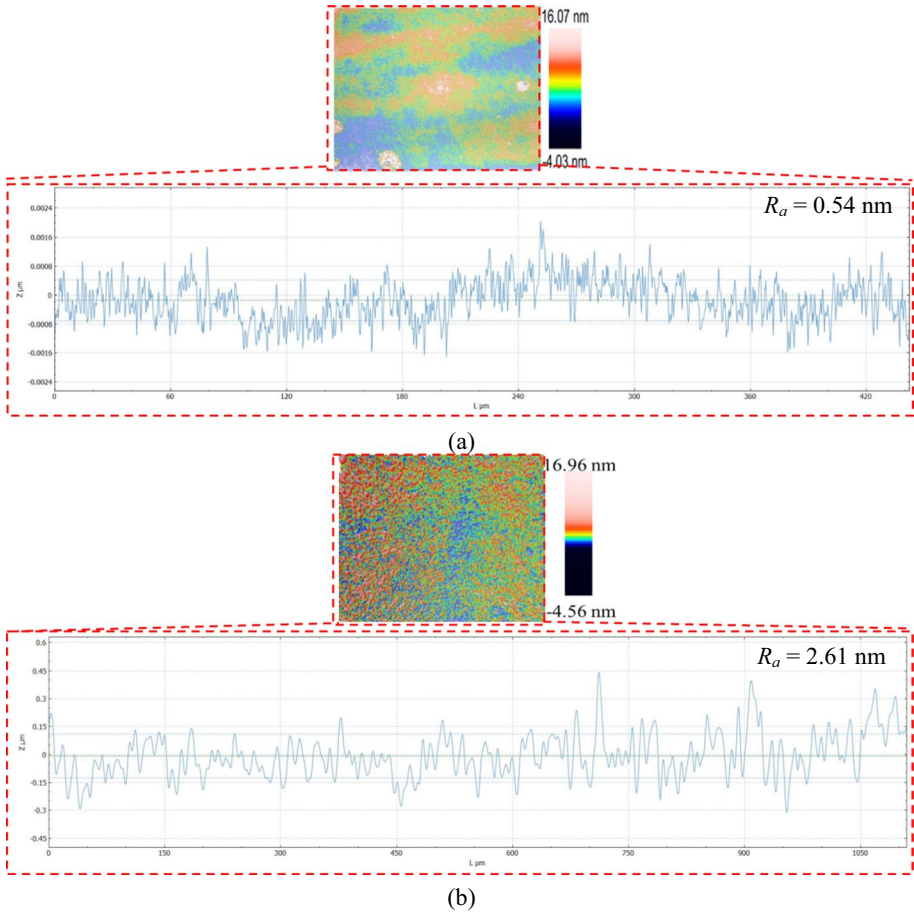
The spatial distribution and consistency of chemically reactive radicals in the plasma chamber will strongly influence surface roughness and material removal. An optical emission spectrometer (OES) is used to monitor the plasma at specific wavelengths. It is a non-invasive spectroscopic method for real-time monitoring during plasma polishing. Plasma polishing experiments are conducted on fused silica prism with varying pressure ratios ( $\text{SF}_6/\text{O}_2$ ) between 1:2 to 3:1 for a total pressure of 5 and 20 mbar with a polishing time of 40 min. Figure 5 illustrates the intensities of activated fluorine atoms (i.e., F atoms) at different wavelengths with varying pressure ratios for a total pressure of (a) 5 and (b) 20 mbar. It is clear that the intensity increases up to 1:1 and then further decreases, especially for the F atom spectrum at a different wavelength. Moreover, the results show the intensity at 5 mbar is higher than 20 mbar. The previous literature also reported that at a wavelength of 685.60 nm, the intensity of excited F atoms reaches its maximum value [23]. The presence of O promotes the dissociation of  $\text{SF}_6$  into  $\text{SF}_5$  and  $\text{F}^*$ , and O associates with  $\text{SF}_5$  preventing the recombination of  $\text{F}^*$  with  $\text{SF}_5$ . Hence, with an increased  $\text{O}_2$  gas flow rate, the removal rate increases. With the further increase in the  $\text{O}_2$  gas flow rate, the generated  $\text{O}^*$  reacts with the fused silica surface to form  $\text{SiO}=\text{SiO}$  aggregates which reduce the intensity of the F atom [24]. The intensity of activated F atoms decreases with increased total pressure, particularly at the wavelength of 685.60 nm. Atoms at 685.60 nm wavelength are most significant in finishing the fused silica materials. This means MRR and surface finish become higher for the activated F atom on the machined surface.

## Comparison Between Plasma Processed and Wet Chemical Etching Surfaces

This section compares the medium-pressure plasma processed and wet chemical etching of a fused silica cuboidal prism to reveal their smoothness, surface roughness, morphology, and topography.



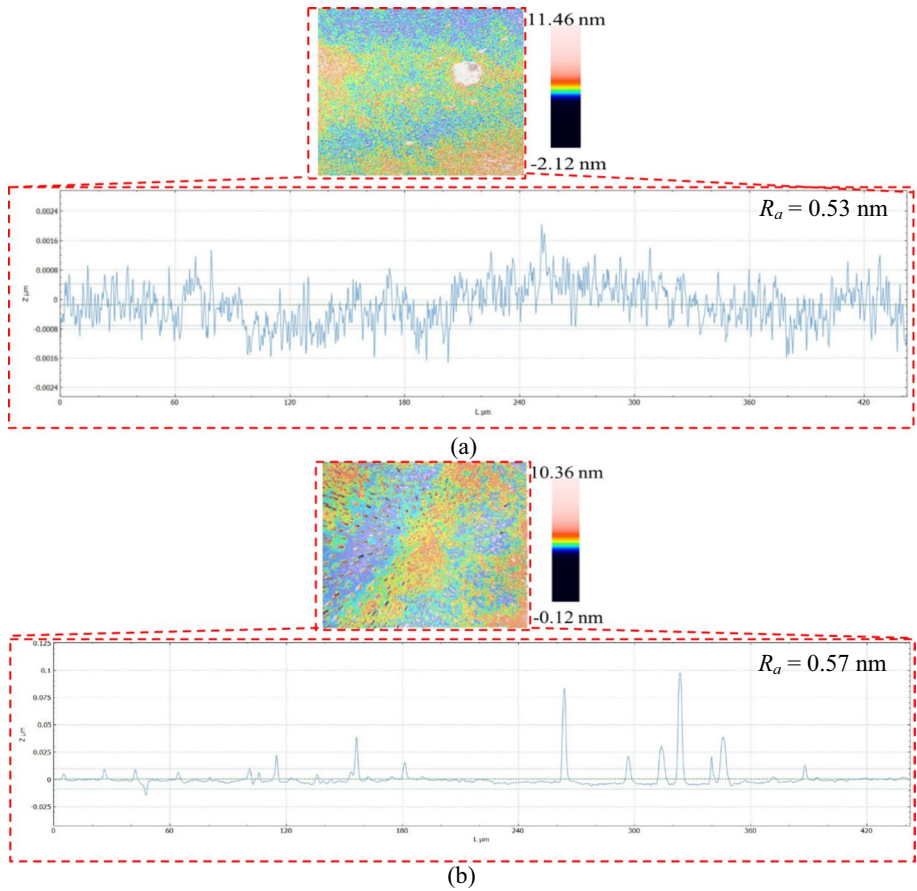
**Fig. 5** Consistency and spatial distribution of activated F atoms at **a** 5 and **b** 20 mbar pressure



**Fig. 6** 2D and 3D profiles **a** before and **b** after plasma processing of fused silica prism at 5 mbar total pressure

### Surface Roughness Analysis

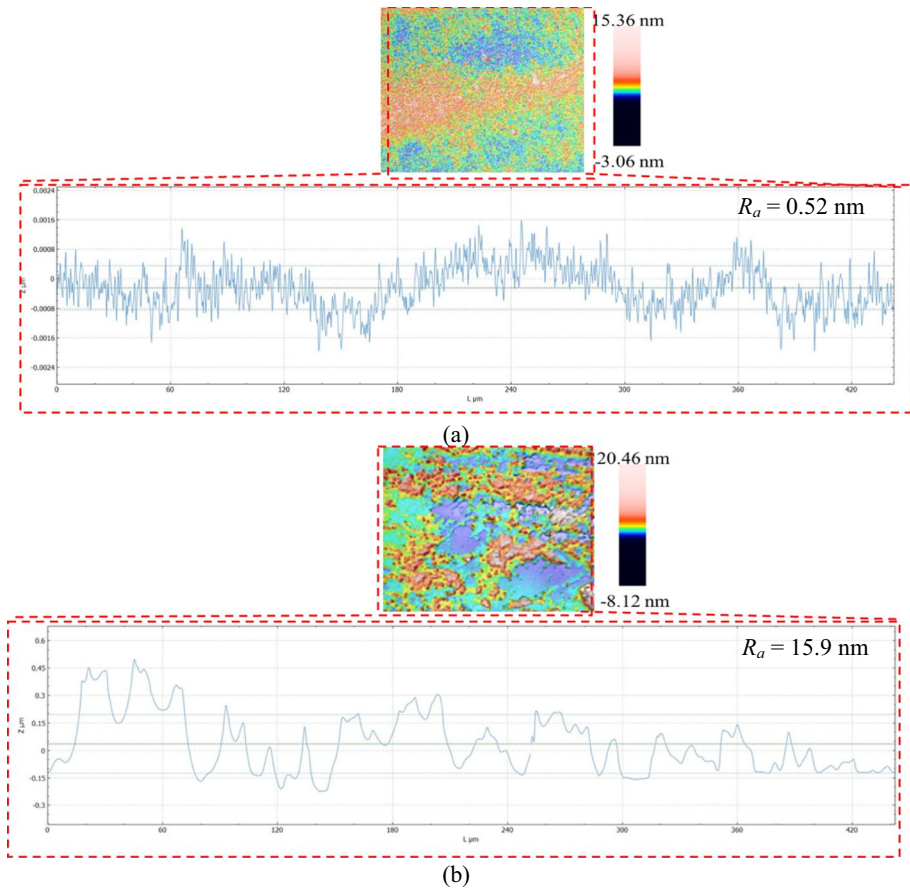
The plasma processing experiments are carried out at optimized process parameters, i.e., 90:10 gas composition, 1:1 pressure ratio, and 80 W RF power. The parameter settings have been chosen based on the preliminary experimental studies [17]. Surface roughness ( $R_a$ ) of  $\text{SiO}_2$  substrate is investigated before and after the plasma polishing with a polishing time of 40 min. Figure 6a and b show the  $R_a$  profiles before and after plasma processing, respectively, at 5 mbar. The results in Fig. 6 depict that the surface roughness value increases from its initial value of 0.54 nm after plasma polishing. During processing, the chemical reaction occurs between fluorine radicals ( $\text{F}^*$ ) and fused silica surface atoms, which removes material from the substrate. Moreover, a physical bombardment of radicals and ions with substrate surface atoms also happens during processing at lower pressure, i.e., 5 mbar. The 3D surface image/topography and 2D surface roughness profile are obtained using a 3D optical profilometer, as illustrated in Fig. 6.



**Fig. 7** 2D and 3D profiles **a** before and **b** after plasma processing of fused silica prism at 20 mbar total pressure

Figure 7a and b show area surface roughness profiles ( $R_a$ ) before and after the plasma processing of fused silica substrate, respectively, for 20 mbar total pressure. The surface roughness increases from an initial value of 0.53 to 0.57 nm after plasma processing. Each sample's measurements are repeated three times, and the mean roughness value is further calculated. The 3D surface image and 2D surface roughness profiles are illustrated in Fig. 7. The surface roughness is much higher at 5 mbar total pressure than 20 mbar because of the high energy of species reacting with surface atoms. The plasma polished surface displays reduced defects and surface cracks after plasma processing because the fluorine radicals come into contact with the surface, and  $F^*$  radicals react with micro-cracks sidewalls. Gradually, the etched holes begin to intersect and merge. The surface roughness changes to irregular concave-convex shapes once the isolated pits coalesce. Microcracks and bond strain become eliminated, but surface topography changes after the plasma process. Consequently, micro-cracks and etched pits are diminished following the plasma processing.

Further wet chemical etching has been performed under the solution of HF and  $H_2SO_4$  for 2 min etching time. Preliminary experiments are conducted to remove material using wet chemical etching. The removal depth of material is controlled with



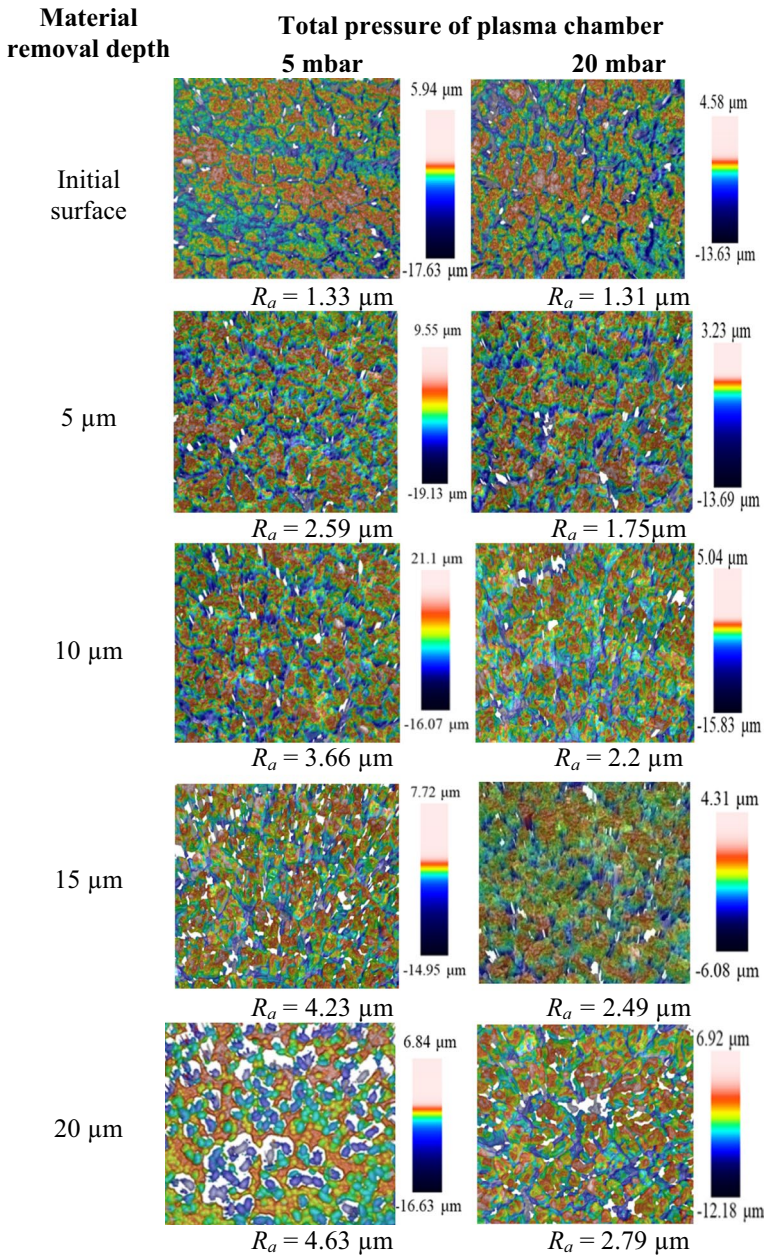
**Fig. 8** 2D and 3D surface roughness profiles **a** before and **b** after wet chemical etching of fused silica prism

processing time, and it has been known from the preliminary experiments. Figure 8a and b illustrate the initial and final surface profiles before and after wet chemical etching.

The result reveals that the surface roughness increases from its initial value of 0.52 to 15.9 nm after wet chemical etching. Moreover, the scratches are enlarged, and the microcracks open up and become blunt due to wet chemical etching. The initial area surface roughness ( $R_a$ ) value on fused silica substrate increases after wet chemical etching because of the uncontrolled chemical reactions. Wet etching severely damages the substrate's surface topography while eliminating microcracks. Although microcracks and bond strain are reduced, surface topography changes. The 3D surface image/topography and 2D surface roughness profiles are obtained after wet chemical etching using a 3D optical profilometer, as illustrated in Fig. 8.

Figure 9 shows the surface topography of fused silica at various material removal depths and total pressures. Due to the limited number of costly substrates, i.e. prism, these experiments (i.e., investigation of surface topography at different material removal depths) are performed on plane fused silica substrate. The result depicts that surface roughness





**Fig. 9** Images of fused silica surface topography after plasma polishing at different pressures with material removal depth

increases with the material removal depth, i.e., between 5 and 20  $\mu\text{m}$  at a total pressure of 5 mbar. Similar results are also observed at 20 mbar, but the % change in surface roughness (i.e.,  $\% \Delta R_a$ ) at 20 mbar is lower than the 5 mbar.

**Fig. 10** Surface topography images of fused silica substrates **a** initial and **b** after wet chemical etching

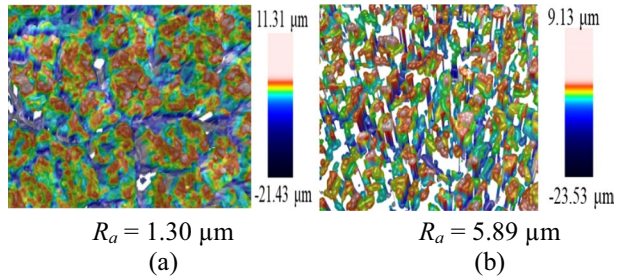
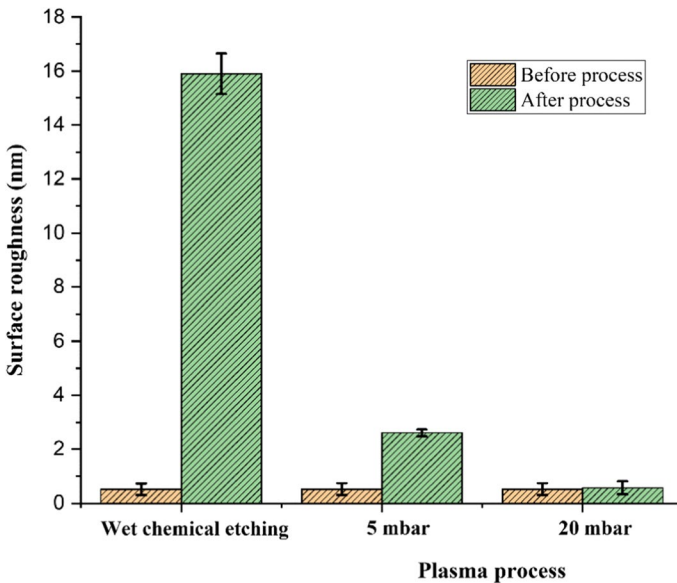


Figure 10 shows the surface topography images of fused silica substrates (a) initial and (b) after wet chemical etching. The initial fused silica substrates are prepared on a lapping machine, followed by ultrasonic cleaning, and dried with nitrogen to achieve the required surface conditions. The substrates are processed up to 20 μm material removal depth on a similar initial surface using wet chemical etching. The results show that the surface roughness value increases to 5.89 μm from the initial value of 1.30 μm. However, wet chemical etching shows higher surface roughness on the substrate surface than the plasma process. Hence, wet chemical etching is recommended when a higher material removal rate is desired, regardless of surface roughness.

The cuboidal-shaped fused silica prism substrates are investigated using medium-pressure plasma and wet chemical etching. The plasma process has been performed at 5 and 20 mbar, 80 W RF power, for a machining time of 40 min. Hawat and Akel [25] reported that with increasing the pressure, at a constant power, the intensity decreases especially in the middle part of the discharge. The increased surface roughness after plasma processing is higher at 5 mbar total pressure than 20 mbar due to the higher energy ions and radicals



**Fig. 11** Comparison between surface roughness values of substrates before and after wet chemical etching and plasma processing at different pressures



at low pressure; thus, a smooth surface has been observed at higher pressure, i.e., 20 mbar. Moreover, wet chemical etching is performed in the solution of HF and H<sub>2</sub>SO<sub>4</sub> for 2 min etching time. The results show that the surface roughness becomes higher in wet chemical etching than in the plasma process for both 5 and 20 mbar total pressures. The comparison of surface roughness values between the plasma process and wet chemical etching is illustrated in Fig. 11.

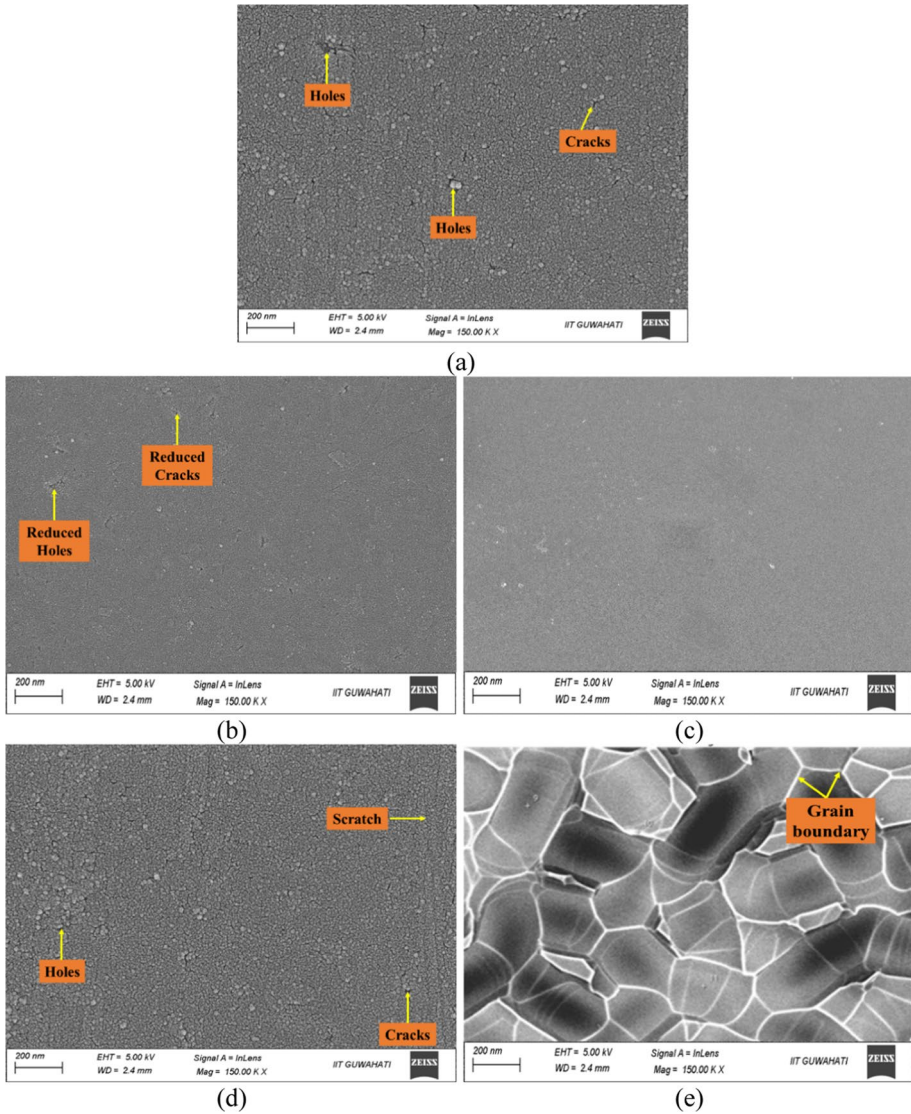
However, wet chemical etching offers simplicity, cost-effectiveness, and higher material removal. Wet etching consistently leads to a significant degradation of surface topography while eliminating microcracks. Microcracks and bond strain are eliminated [26]; however, surface topography changes. It is concluded that the plasma polishing process provides anisotropic etching, which means it etches vertically rather than isotropically. This allows for precise control over the etching profile. However, wet chemical etching allows for faster material removal during fabrication.

### Analysis of Surface Morphology and Elemental Composition

FESEM analysis is a powerful imaging technique used to obtain high-resolution, detailed images of the surface morphology and topography of a wide range of materials. The surface morphology of fused silica (i.e., optical material) before and after the plasma process and wet chemical etching are shown in Fig. 12. Figure 12a shows surface morphology before plasma processing, and Fig. 12b and c show the surface morphology after plasma processing at 5 and 20 mbar total pressure, respectively. The surface morphology in Fig. 12b shows that the microstructure becomes refined and regular, and the cracks are reduced after plasma processing at 5 mbar total pressure. A similar result is also observed at 20 mbar total pressure, and the cracks have been removed from the surface. Moreover, the results show that the etched pits mostly disappeared after the plasma process at both 5 and 20 mbar pressure.

Figures 12d and e show surface microstructure before and after wet chemical etching. Some cracks, holes, and scratches are visible on the initial surface (Fig. 12d). Also, microstructures are small and regular before processing. The shape of the microstructure and grain boundary has been enlarged and visible after wet chemical etching. The FESEM results show that the grain size (Fig. 12e) is large and is irregular after wet chemical etching, i.e., showing a typical wet chemical-etched surface. The results reveal that the wet chemical method produces etched pits that merge and change into irregular convex-concave structures with deteriorated roughness.

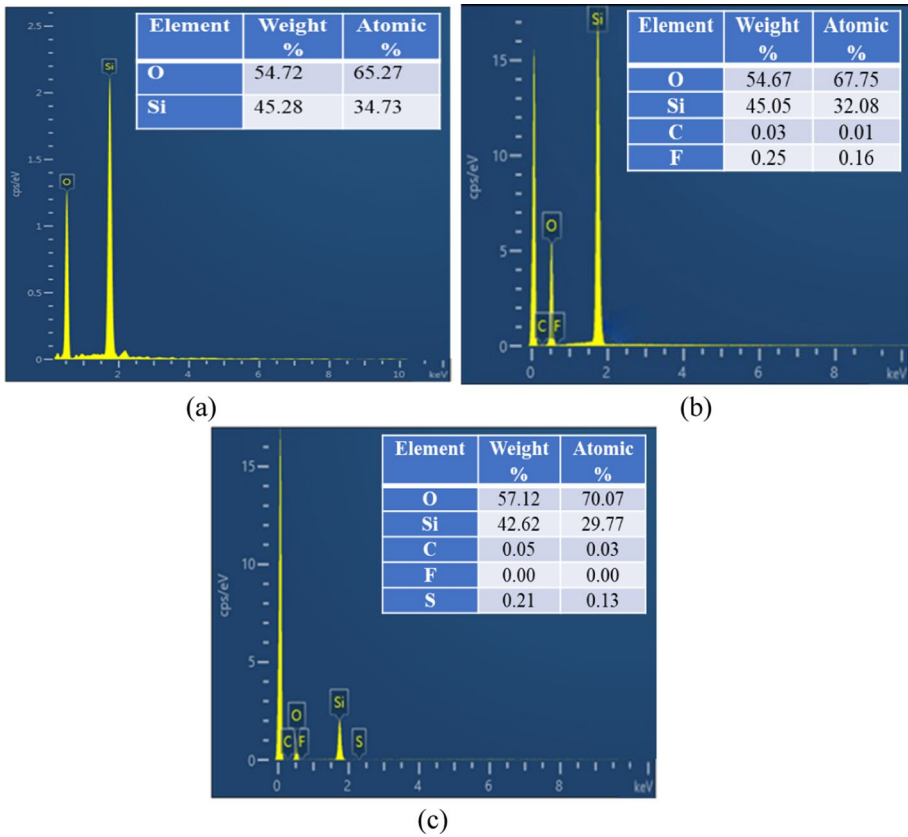
EDX analysis is a technique used to reveal the elemental composition of the substrate. Figure 13 shows the elemental analysis of fused silica using the plasma process and wet chemical etching. Figure 13a, b, and c also give the weight % and atomic % of different elements for plasma polished and wet chemical etched surfaces, respectively. Figure 13a shows the two elements, i.e., O and Si, are present on an initial fused silica sample. After processing, the plasma-processed surface shows the elements, i.e., Si, F, O, and C, as illustrated in Fig. 13b. The additional F element is due to the reaction that occurred with the substrate surface. However, the C element comes from the atmosphere and the O ring. After wet chemical etching, the etched substrate shows the presence of Si, O, F, S, and C elements, as illustrated in Fig. 13c. The additional element, sulfur (S), is observed on the substrate surface after wet chemical etching due to the chemical reactions that happened while processing with the substrate.



**Fig. 12** FESEM images of the substrate **a** initial surface and plasma polished substrate at **b** 5 mbar and **c** 20 mbar pressures; **d** before and **e** after wet chemical etching

### Atomic Force Microscopy Analysis

Atomic force microscopy (AFM) analysis is a powerful imaging technique used to study materials’ surface topography, roughness, and other surface properties. The surface topography of the substrate before and after the plasma processing and wet chemical etching (as illustrated in Fig. 14a–d, are investigated using atomic force microscopy. Figure 14a and c depict the initial surface topography of the substrate before processing. Figure 14b shows the surface topography of fused silica without any surface defect or contamination

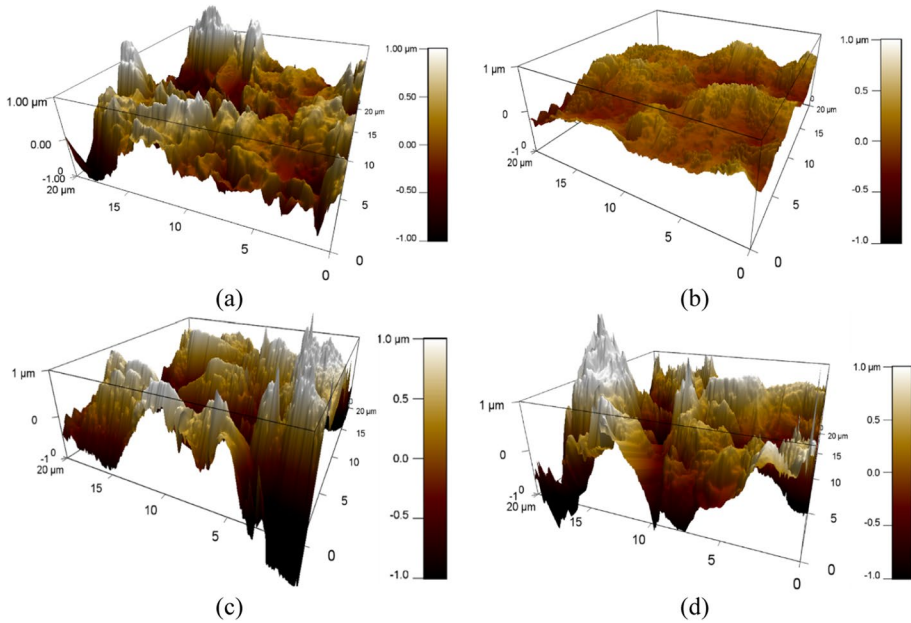


**Fig. 13** EDX images of fused silica prism substrates **a** on the initial surface, after **b** plasma processing, and **c** wet chemical etching

using the plasma process at 20 mbar total pressure. Also, the roughness peaks are reduced (Fig. 14b) after plasma processing than the initial surface (Fig. 14a). However, the roughness peaks became irregular, and their height increased after wet chemical etching, as illustrated in Fig. 14d compared to the initial surface (Fig. 14c). Therefore, the MPPP process has the potential to support the finishing of optical materials to attain ultra-smooth surfaces.

### Raman Spectroscopy Analysis

The practical approach for determining the structural change in fused silica is Raman spectroscopy [27]. Raman spectroscopy reveals broad bands that correspond to the linked vibration modes of  $\text{SiO}_2$  network [28]. The silica network's Raman peak (1), at  $490 \text{ cm}^{-1}$ , connects to the Si–O–Si angle, and its breadth and area imply the Si–O–Si angle distribution [29]. The silicon dioxide network is preferably a six-member structure (as illustrated in Fig. 15a). It is converted into 3 and 4 – members during the contact machining process (as shown in Fig. 15b and c). The emergence of two distinct bands, one centered at  $490 \text{ cm}^{-1}$  and the other at  $605 \text{ cm}^{-1}$ , can be attributed to the in-phase breathing motion of oxygen



**Fig. 14** AFM images of substrates **a** before and **b** after plasma polishing at 20 mbar total pressure; **c** before and **d** after wet chemical etching

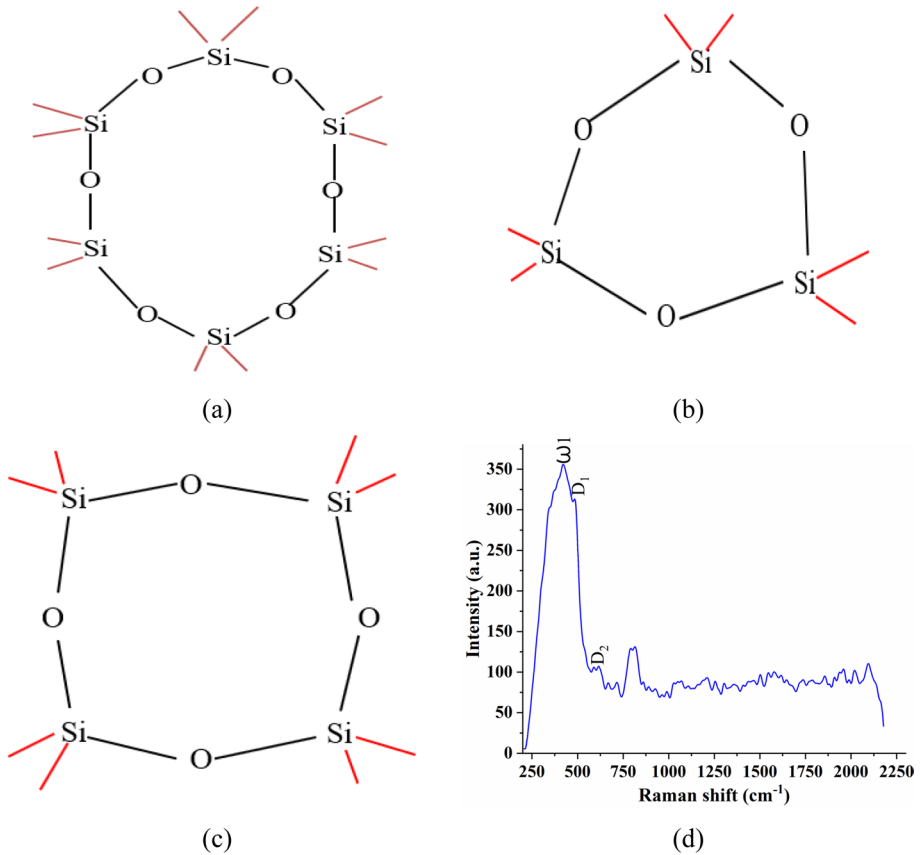
atoms within puckered structures of both four- and three-membered rings [30]. After processing, Fig. 15d displays the spectra containing  $D_1$  and  $D_2$  as defect lines at 490 and 605  $\text{cm}^{-1}$  wavelengths, respectively.

Figure 16 compares the substrate surface area under the 490  $\text{cm}^{-1}$  and 605  $\text{cm}^{-1}$  peaks before and after plasma processing. The improvement in the ratio of the peak at 490 to 605  $\text{cm}^{-1}$  (until 10  $\mu\text{m}$  material removal depth) from 1.52 to 2.82 shows the sub-surface defects and strained layers have been reduced.

## Conclusions

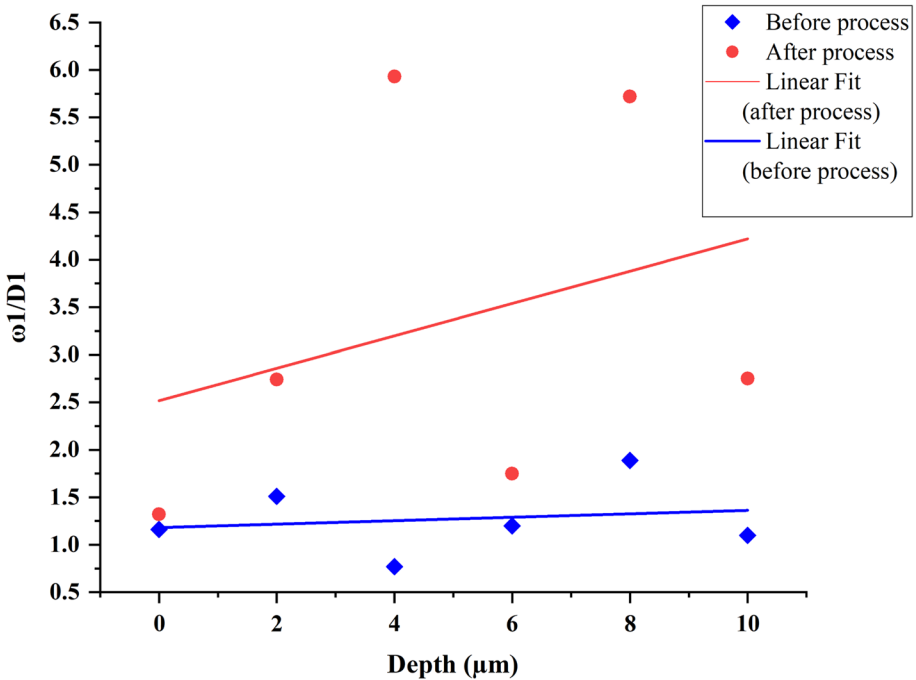
The polishing techniques, i.e., medium-pressure plasma process and wet chemical etching, are proposed to obtain a smooth surface finish without introducing defects and subsurface damage. This article emphasizes a comparative study of surface roughness in medium-pressure plasma processes and wet chemical etching. The surface roughness, morphology, elemental composition, and surface topography are investigated and analyzed using a 3D optical profiler, FESEM, EDX, and AFM. The following are the primary conclusions:

- The surface roughness ( $R_a$ ) is slightly improved from 0.54 to 2.61 nm (i.e., 5 mbar) and 0.53 to 0.57 nm (at 20 mbar); utilizing MPPP ensures the absence of surface contamination. A higher surface roughness ( $R_a$ ) value is observed at 5 mbar total pressure than 20 mbar. It is caused due to the more excitation and ionization of ions inside the plasma chamber at 5 mbar. The molecules achieved higher energy at low pressure than at higher pressure.



**Fig. 15** Schematic of **a** 6-membered, **b** 3-membered, **c** 4-membered structures, and **d** spectrum of fused silica

- 2D and 3D surface roughness are measured before and after wet chemical etching. The results show that  $R_a$  is increased from an initial value of 0.52 to 15.9 nm after etching..
- FESEM results show that the grain size got reduced and remained regular in shape after plasma processing. However, the grain size became very fine at 20 mbar total pressure than 5 mbar. Also, irregular and larger grain boundary is observed after wet chemical etching.
- EDX results show the reaction involved during the plasma process and wet chemical etching. The additional elements F, C, and sulfur (S) are observed after the plasma processes and wet chemical etching. It shows the reactions that happened while processing with the substrate.
- AFM result shows that MPPP has reached an outstanding surface topography of optical material without any surface defect or contamination. The results show the surface topography peak is reduced after the plasma process. However, a higher increase in surface roughness peak is observed in the case of wet chemical etching.
- The improvement in the ratio from 1.52 to 2.82 shows the sub-surface defects and strained layers have been reduced using Raman spectroscopy analysis.



**Fig. 16** Comparison of the substrate surface area under the peaks at  $490\text{ cm}^{-1}$  and  $605\text{ cm}^{-1}$  before and after plasma processing

**Acknowledgements** We thank the Science and Engineering Research Board, New Delhi, India, for its financial support of project No. E.C.R./2018/002801 titled "Design and development of a novel plasma processing set up for uniform nanopolishing of prism and any freeform surfaces of fused silica."

**Authors' Contributions** HNSY: Conceptualization, Methodology, Data curation, Investigation, Writing—review & editing. MD: Supervision, Writing—review & editing.

**Data Availability** Data will be made available on request.

## Declarations

**Competing interests** The authors declare no competing interests.

## References

- Narayan H, Yadav S, Das M (2023) Experimental investigations through modeling and optimization for fabrication of fused silica in medium-pressure plasma process. *Opt Mater* 143:114157
- Yadav HNS, Das M (2023) Surface characteristics of fused silica in medium-pressure plasma process. *Mater Today Proc* 1–5
- Yadav HNS, Kumar M, Kumar A, Das M (2021) Plasma polishing processes applied on optical materials: a review. *J Micromanufacturing* 6:251659842110388
- Kogelschatz U (2003) Dielectric-barrier discharges: their history, discharge physics, and industrial applications. *Plasma Chem Plasma Process* 23:1–46
- Yadav HNS, Kumar M, Das M (2022) Fundamentals of plasma polishing. In: Jain VK (ed) *Advanced machining science*. CRC Press, Boca Raton, pp 203–228
- Schindler A and Boehm G and Haensel T and Frank W and Nickel A and Rauschenbach B and Bigl F (2001) Precision optical asphere fabrication by plasma jet chemical etching (PJCE) and ion beam figuring. In: *Optical manufacturing and testing*. p 242–248



7. Zhang J, Wang B, Dong S (2008) Analysis of factors impacting atmospheric pressure plasma polishing. *Int J Precis Eng Manuf* 9:39–43
8. Dev DSD, Krishna E, Das M (2019) Development of a non-contact plasma processing technique to mitigate chemical network defects of fused silica with life enhancement of He–Ne laser device. *Opt Laser Technol* 113:289–302
9. Yadav HNS, Kumar M, Kumar A, Das M (2021) COMSOL simulation of microwave plasma polishing on different surfaces. *Mater Today Proc* 45:4803–4809
10. Gerhard C, Weihs T, Luca A et al (2013) Polishing of optical media by dielectric barrier discharge inert gas plasma at atmospheric pressure. *J Eur Opt Soc* 8:1–5. <https://doi.org/10.2971/jeos.2013.13081>
11. Arnold T, Boehm G, Mueller H, et al (2022) Plasma jet assisted polishing of fused silica freeform optics. In: European physical journal web of conferences. p 03001
12. Gerhard C, Weihs T, Tasche D et al (2013) Atmospheric pressure plasma treatment of fused silica, related surface and near-surface effects and applications. *Plasma Chem Plasma Process* 33:895–905
13. Arnold T, Boehm G, Paetzelt H (2015) New freeform manufacturing chain based on atmospheric plasma jet machining. In: Freeform optics. p FTh1B.3
14. Li R, Li Y, Deng H (2022) Plasma-induced atom migration manufacturing of fused silica. *Precis Eng* 76:305–313
15. Suratwala T, Steele W, Wong L et al (2015) Chemistry and formation of the beilby layer during polishing of fused silica glass. *J Am Ceram Soc* 98:2395–2402. <https://doi.org/10.1111/JACE.13659>
16. Dev DSD, Krishna E, Das M (2016) A novel plasma-assisted atomistic surface finishing on freeform surfaces of fused silica. *Int J Precis Technol* 6:262
17. Narayan H, Yadav S, Krishna E et al (2023) Investigation of MRR and surface characterization using plasma process. *Mater Manuf Process* 38:1–13
18. Narayan H, Yadav S, Das M (2023) Parametric optimisation of plasma polishing process using response surface methodology. *Surf Eng* 39:1–14
19. Feit MD, Suratwala TI, Wong LL et al (2009) Modeling wet chemical etching of surface flaws on fused silica. *Laser-Induced Damage Opt Mater* 7504:75040L. <https://doi.org/10.1117/12.836912>
20. Cheng J, Wang J, Hou J et al (2017) Effect of polishing-induced subsurface impurity defects on laser damage resistance of fused silica optics and their removal with HF acid etching. *Appl Sci* 7:1–23. <https://doi.org/10.3390/app7080838>
21. Ye H, Li Y, Yuan Z et al (2015) Laser induced damage characteristics of fused silica optics treated by wet chemical processes. *Appl Surf Sci* 357:498–505. <https://doi.org/10.1016/j.apsusc.2015.09.065>
22. Ye H, Li Y, Yuan Z, Zhang Q (2018) Ultrasonic-assisted wet chemical etching of fused silica for high-power laser systems. *Int J Appl Glas Sci* 9:288–295. <https://doi.org/10.1111/ijag.12332>
23. Yao YX, Wang B, Wang JH, Jin HL, Zhang YF, Dong S (2010) Chemical machining of Zerodur material with atmospheric pressure plasma jet. *CIRP Ann* 59:337–340
24. Wang D, Liu W, Wu Y et al (2011) Material removal function of the capacitive coupled hollow cathode plasma source for plasma polishing. *Phys Procedia* 19:408–411
25. Al-Hawat S, Polonica MA (2010) Spatial structure of emission intensity in capacitive RF discharge of He: Ne mixture at moderate pressures. *Acta Phys Pol* 117:911–916
26. Dev DSD, Enni K, Das M (2018) Novel Finishing process development for precision complex-shaped hemispherical shell by bulk plasma processing. In: Precision product-process design and optimization. pp. 313–335
27. Xu S, Zu X, Jiang X et al (2008) The damage mechanisms of fused silica irradiated by 355 nm laser in vacuum. *Nucl Instrum Method Phys Res Sect B Beam Interact with Mater Atoms* 266:2936–2940
28. Galeener FL, Leadbetter AJ, Stringfellow MW (1983) Comparison of the neutron, Raman, and infrared vibrational spectra of vitreous SiO<sub>2</sub>, GeO<sub>2</sub>, and BeF<sub>2</sub>. *Phys Rev* 8:15
29. Galeener FL, Geissberger AE (1983) Vibrational dynamics in Si<sub>3</sub>O-substituted vitreous SiO<sub>2</sub>. *Phys Rev B* 27:6199–6204
30. Liu F, Qian J, Wang X et al (1997) UV irradiation-induced defect study of glasses by Raman spectroscopy. *Phys Rev B—Condens Matter Mater Phys* 56:3066–3071

**Publisher's Note** Springer Nature remains neutral with regard to jurisdictional claims in published maps and institutional affiliations.

Springer Nature or its licensor (e.g. a society or other partner) holds exclusive rights to this article under a publishing agreement with the author(s) or other rightsholder(s); author self-archiving of the accepted manuscript version of this article is solely governed by the terms of such publishing agreement and applicable law.